UDC 629 . 11 . 012 . 75

Technical Report

Advanced Evaluation Technologies of Material Properties for Design of Car Body with Enhanced Crash Safety

Satoshi HIROSE* Akihiro UENISHI
Shigeru YONEMURA Shunji HIWATASHI

Abstract

The accuracy of crash analysis is important for design of car body with crashworthiness and depends on some properties of applied material. Strain rate dependency of flow stress and bake hardenability caused by painting process of car body are of particular significance to crash analysis. Here, developed technologies for evaluation of their properties were introduced.

1. Introduction

To enhance collision safety and reduce CO_2 emission simultaneously, ultra-high-strength steel sheets of tensile strength exceeding 1,500 MPa, suitable for hot stamping and similar working, are widely used for automotive structural parts. However, collision safety is determined not only by tensile strength but also by factors related to all the processes from manufacture, shipment, working of the steel materials, assembly into car bodies, painting, and the mode of collision. For this reason, when ultra-high-strength steels are used, collision safety design must take into consideration a wide variety of aspects beyond the simple substitution of a material with another.

Collision analysis applying general-purpose software programs of the finite element method (such a program is hereafter referred to as a FEM program) are widely employed for collision safety evaluation at design stages. Recently, the application of FEM simulation has expanded from the deformation behavior of car bodies at collision to the fracture of base metal [1, 2] as well as that of weld joints; [1, 3] as a result, the prediction accuracy of collision safety has been enhanced significantly. According to common fracture prediction methods,[4, 5] the occurrence or otherwise of fracture is judged on the basis of expected changes of state variables such as stress and strain. Therefore, the accuracy of fracture prediction depends on the measurement accuracy of the stress-strain curve, a material property item to input to the prediction program. In addition, since measurement data are used in the form of material models in collision analysis, it is necessary to select adequate material models based on real material properties and the characteristics of different measurement methods employed.

In consideration of the above, the present paper reports the results of fundamental studies on the strain rate sensitivity of flow stress, a material property item important in collision analysis, and on work hardening under press forming and bake hardening in the painting process of car bodies. Section 2 deals with studies on the shape of test pieces for a high-speed tensile test adequate for accurately evaluating the strain rate sensitivity. Section 3 describes the mechanism through which the sensitivity becomes manifest and studies on material models appropriate for collision analysis. Section 4 describes the anisotropy of the yield stress of steel sheets under press forming, painting, and baking.

2. Method of Evaluating Material Properties of Ultra-high-strength Steels in a High-strain-rate Range

Material properties figures are important for accurately evaluating collision performance of car bodies through analysis, particularly the result (the stress-strain curve) of the tensile test at a high strain rate (1,000 s^{-1}), i.e., approximately a million times that of common tensile test.[6] It is necessary to increase the tension speed using a hydraulic servo or a similar hydraulic device to achieve such a high strain rate, but that alone is not enough for improving measurement accuracy satisfactorily.[7]

To evaluate stress imposed on a test piece with high precision, it is necessary to introduce a load measurement method,[8, 9] such as the

* Senior Researcher, Ph.D., Forming Technologies R&D Center, Steel Research Laboratories
20-1 Shintomi, Futtsu, Chiba 293-8511

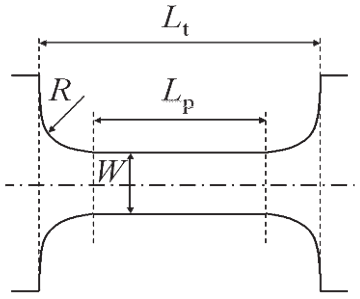

Fig. 1 Specimen geometry

elastic bar method, that takes into consideration the fact that stress propagates as deformation waves as a result of the elasto-plastic deformation of the effective part of a test piece and the elastic deformation of its other parts.[10] In this relation, note that stress is calculated by dividing the load during measurement by the initial sectional area of the test piece. In addition, note that the evaluation method of strain is different depending on the restrictions of the test method applicable; for instance, by the elastic bar method, strain is calculated mostly on the basis of the elongation of a test piece caused by the difference in the measured displacement of bar ends.[9]

On the other hand, stress and strain were measured or calculated in a high-strain-rate range change depending on the test piece geometry.[11] Furthermore, although the effects of the propagation of deformation waves or that of stress waves can be disregarded in a low-strain-rate range, whereas, it is impossible to disregard them in a high-strain-rate range.[12] In view of this, through simulation, the authors studied the test piece geometry for the stress-strain evaluation of steel sheets with high accuracy, and defined the test piece length L_t, parallel length L_p, width W, and shoulder radius R (see **Fig. 1**).[13] In consideration of the fact that the propagation velocity of stress wave changes depending on material properties, they also studied the effects of material properties.[14]

2.1 Analysis conditions

The high-speed tensile test by the elastic bar method was simulated using a general-purpose dynamic explicit FEM program.[15] Test pieces of different geometries given in **Table 1** (see also Fig. 1) were used as models. Boundary conditions were set so as to simulate the real high-speed tensile test by the elastic bar method.[13, 14] Furthermore, Swift- and Cowper-Symonds-type constitutive equations were adopted (Equation (1), where σ is the stress, ε_p is the plastic strain, and ε_v is the strain rate (s^{-1})). Steel sheets of a 980-MPa class tensile strength (α in **Table 2**) and those of a 590-MPa class tensile strength, but significantly different in terms of work hardenability (β of high work hardenability, and γ of low work hardenability in Table 2) were chosen as specimens. In addition, to confirm the adequateness of the selected test piece geometry, the same simulation of tensile test was conducted considering a material equivalent to ultra-high-strength steel (δ in Table 2). Note that the tensile strength and the uniform elongation expected for material δ are approximately 1,640 MPa and 0.05, respectively.

$$\sigma = K(\varepsilon_0 + \varepsilon_P)^n \left(1 + \left(\frac{\varepsilon_V}{X}\right)^{\frac{1}{Y}}\right) \quad (1)$$

where K, ε_0, n, X, and Y are material parameters (see Table 2).

2.2 Conditions of test pieces required for the high-speed tensile test

In order to study the geometry of test pieces for the high-speed tensile test by the elastic bar method following four conditions must be satisfied.

Condition I : the state of uniaxial stress is maintained.
Condition II : an equilibrium condition is attained quickly.
Condition III : necking at positions other than the center in an early stage must be avoided.
Condition IV : the shoulder radius R must be such that uneven deformation is minimized.

Condition I applies also to test pieces for the tensile test in a low-strain-rate range; Fukui et al. studied optimum conditions regarding this point.[16, 17] From the analysis result, the present study confirmed that Condition I was equally essential in a high-strain-rate range; in addition, it confirmed that, when the parallel length L_p and the width W satisfy Equation (2), stress in the width direction can be virtually disregarded and the state of uniaxial stress in the longitudinal direction would be attained.[14] The other conditions apply only to test pieces for the high-speed tensile test; Conditions II and III depend on the propagation velocities, respectively, of elastic and plastic waves,[18] both of which are stress waves, and the propagation of stress waves must be taken into consideration for the tensile test in a high-strain-rate range.

Condition II accelerates the transmission and reflection of elastic waves and makes the distribution of tensile load substantially even within a test piece. It is considered that the smaller the distance of elastic wave propagation or the test piece length L_t, the better; the result of the present study also corroborated this. This means that the relationship shown in Equation (3) is important.[14] Condition III, on the other hand, requires that concentration of deformation, which inevitably occurs at positions other than the test piece center at an initial stage of deformation owing to the restrictions of test piece shape, is transferred to the center during the deformation process. When the transfer is too slow, deformation concentrates locally at the initial position, necking occurs away from the center, leading to a significant underestimation of uniform elongation.[12, 19]

Fig. 2 shows the change in the distribution of equivalent plastic strain in the simulated tensile test in the cases where the ratio of the width to parallel length W/L_p of test pieces was 3.4 and 5.7; the analysis shows that when the test piece shape is inadequate, necking occurs near an end instead of the center.[19] Therefore, it follows that it is necessary to bring the position of initial deformation concentration as close to the center as possible in consideration of the fact that the propagation speed of plastic waves is far lesser than that of elastic waves. The analysis confirmed that, to satisfy Condition III, it was necessary to satisfy Equation (4), which is the same as Equation (2) except that the inequality sign is reversed.[14] Condition IV is unique to the tensile test by the elastic bar method. Because of the

Table 1 Specimen geometries

Thickness (mm)	L_t (mm)	W (mm)	R (mm)
1.4	10 - 90	3 - 12.5	0.5 - 25

Table 2 Material parameters

Material	K (MPa)	ε_0	n	X (s^{-1})	Y
α	1,650	0.0004	0.14	3.40×10^{11}	6.4
β	1,050	0.0020	0.22	5.00×10^{6}	4.0
γ	900	0.0020	0.12	6.00×10^{7}	5.0
δ	2,000	0.0001	0.05	5.00×10^{12}	7.0

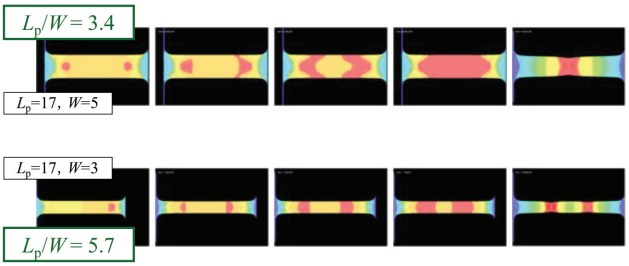

Fig. 2 Test piece geometry and distribution history of equivalent plastic strain

limited following ability of the extensometer,[20] the dislocation of bar ends including the shoulders is often regarded as elongation. Therefore, it is necessary to define test piece geometry such that, for engineering purposes, the effects of strain unevenness originating from the shoulders can be disregarded. From the analysis, the authors confirmed that measured figures agreed with actual material properties considerably well when Equation (5) was satisfied.[14]

Condition I : $L_p/W \geq C_I$ (2)

Condition II : $L_t \leq C_{II}$ (3)

Condition III : $L_p/W \leq C_{III}$ (4)

Condition IV : $C_{IVa} \leq R/L_t \leq C_{IVb}$ (5)

It should be noted that the threshold values C_I, C_{II}, C_{IVa}, and C_{IVb} of Conditions I, II, and IV do not change significantly depending on material properties as far as the subject materials α, β, and γ of the present study are concerned, but the threshold value C_{III} of Condition III changes depending on the material. Because Condition III relates to the propagation speed of plastic waves, the difference is presumably attributable to the difference in work hardenability.[14] Since the work hardenability of ultra-high-strength steels, the use of which has rapidly grown over the last years, is generally poor, it is necessary for the tensile test of this type of steel in a high-strain range to select a test piece shape that satisfies Condition III.

2.3 Test piece shape most suitable for the high-speed tensile test and its applicability to ultra-high-strength steels

Assuming the threshold values C_I, C_{II}, C_{III}, C_{IVa}, and C_{IVb} of Equations (2)-(5) to be 1.4, 10, 2, 0.07, and 0.12, respectively, the optimum test piece shape falls within the hatched area in **Fig. 3**. Note that the threshold values assume a critical machining value of the shoulders of 1.0 mm and steel having very low work hardenability; therefore, the range is practically achievable with steels for hot stamping, the use of which has increased recently.

Furthermore, to confirm the applicability of the defined optimum test piece shape to ultra-high-strength steels, simulation of the high-speed tensile test was conducted with respect to the material equivalent to ultra-high-strength steel sheets (δ in Table 2). Here, the test piece geometry was set within the hatched area in Fig. 3 as follows: L_t (= L_p + 2R) = 10.0, W = 4.0, and R = 1.0. **Fig. 4** shows the stress-strain curve predicted by the analysis; the prediction result agreed with the input stress-strain curve within the range up to uniform elongation, which indicates that the test piece shape is applicable to ultra-high-strength steel sheets.

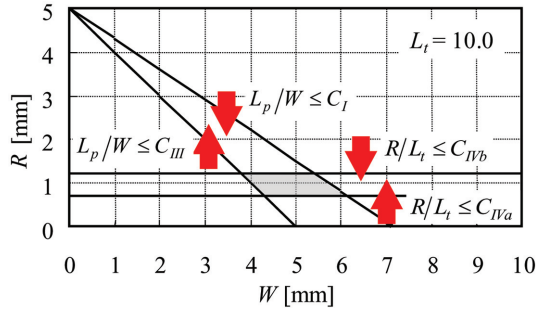

Fig. 3 Area of appropriate specimen geometry

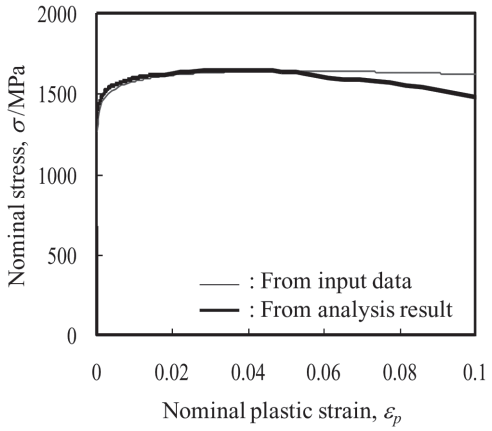

Fig. 4 Stress-strain curves

3. Study of Material Model Adequate for Collision Analysis

A wide variety of materials from mild to ultra-high-strength steels of tensile strengths exceeding 980 MPa have started being used for different parts of automobile bodies to enhance collision safety and reduce CO_2 emission. As stated in Section 2, for improving the accuracy of collision analysis, it is necessary to accurately evaluate the strain rate sensitivity of flow stress of materials. For this reason, the authors first investigated the strain rate sensitivity of flow stress of different steels; then, to clarify the mechanism of the strain rate sensitivity, they studied its relationship with steel strengthening mechanisms. Steel is strengthened generally by introducing some unevenness to the crystal structure; such measures include solid solution hardening, precipitation hardening, refinement of crystal grains, and strengthening by a second phase. Here, the authors focused on ferrite, the main phase of steel sheets for automotive use, and studied the relationship between the strain rate sensitivity of flow stress and structural strengthening.

Large amounts of strain are imposed on various body parts at collision. For this reason, it is necessary to input, as part of analysis conditions, material property data in a wide range of strain rate and up to a high strain region. In the material property measurement by the widely applied simple tension method, necking occurs after uniform elongation; consequently, test pieces fail prematurely, which makes it difficult to evaluate work hardening characteristics in a high-strain range. In consideration of this, the authors attempted to evaluate work hardening characteristics in a high-strain range using methods such as the simple shear test,[21] which is less prone to necking, and the correction of uniaxial tensile test by applying FEM analysis.[22] In addition, they studied the deformation mechanisms of test pieces on the basis of the results of this test and analysis, and examined material models that could adequately express material behavior in collision analysis.[23]

3.1 Evaluation of the strain rate sensitivity of flow stress by the high-speed tensile test

3.1.1 Evaluation of the strain rate sensitivity of specimen sheets

To clarify the mechanism through which the strain rate sensitivity of flow stress becomes manifest, the authors prepared an interstitial-free (IF) steel containing 0.2 mass% Ti; then, they prepared solution-hardened steels by adding Mn or Si of 1 or 2 mass % to the IF steel (see **Table 3**). These steels were hot rolled to a thickness of 2.0 mm; then, annealed at 600°C for 60 min. The strengthening of these steels was mainly due to solution hardening with Mn or Si, although they were somewhat different in terms of crystal grain size.[24)]

First, using test pieces of these model steels, the stress-strain curve was measured in low- and high-strain ranges (0.001 and 1,000 s^{-1}, respectively) by the common tensile test and high-speed tensile test of the one-bar method.[25)] **Fig. 5** shows the relationship between the difference in flow stress at 5% strain at a strain rate of 1,000 $s^{-1}$and 0.001 s^{-1}, and the flow stress at 5% strain at a strain rate of 0.001 s^{-1}. It is clear from the graph that the strain rate sensitivity of flow stress decreases with increasing quasi-static flow stress. This behavior of the strain rate sensitivity is presumably because the Peierls-Nabarro barriers, which formed for crystal structure reasons, changed under influences of strain fields caused by solute atoms, and made dislocation motion easier.[24)]

3.1.2 Evaluation of the strain rate sensitivity of flow stress of different Steels

Specimen sheets of various commercial steels from mild steels to those of 1,180-MPa class tensile strength were subjected to the tensile test in the same manner as mentioned in 3.1.1 above, and the strain rate sensitivity was evaluated. The result is shown in part (a) of **Fig. 6**; here, the round marks (●) represent solution-hardened steels, the square ones (■) represent steels that were considered to consist of a single phase based on hardness measurement,[26)] and the triangular ones (▲) represent those that were considered to consist of two or more phases. It is clear from the graph that, with steels considered to consist substantially of ferrite only and having a flow stress less than 600 MPa, the strain rate sensitivity of flow stress is in good correlation with quasi-static flow stress, but quasi-static flow stress cannot be a good indicator of the strain rate sensitivity with multi-phase, high-strength steels.

Table 3 Chemical compositions of solution hardened steels (mass%)

	C	Si	Mn	Al	Ti
IF	0.0016	–	0.10	0.003	0.015
+1at%Mn	0.0013	0.014	0.97	0.003	0.014
+2at%Si	0.0014	0.98	0.10	0.003	0.019
+4at%Si	0.0012	1.97	0.10	0.004	0.023

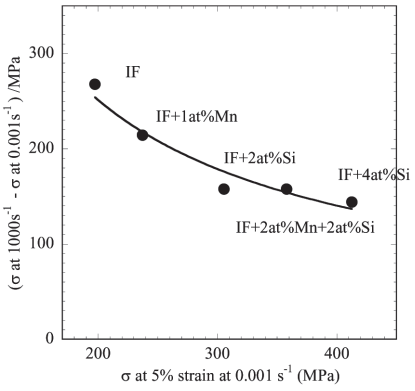

Fig. 5 Strain rate sensitivity of some steels

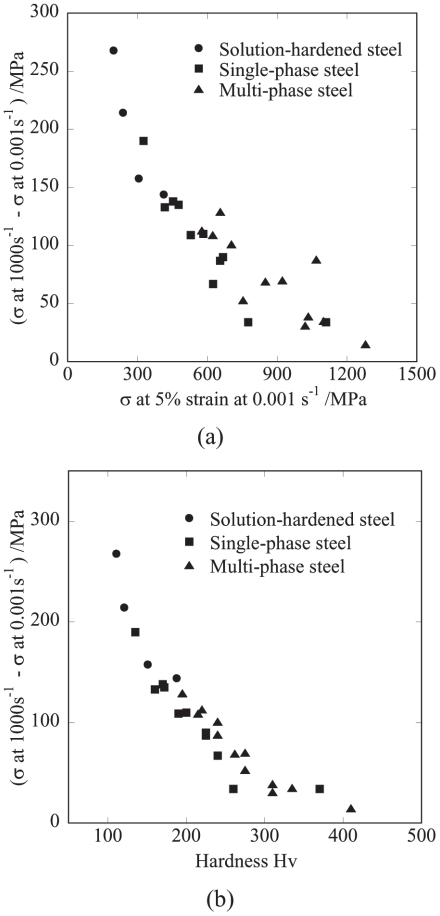

Fig. 6 Strain rate sensitivity of some steels

In this relation, on the basis of hardness measurement, the authors estimated the average hardness of the soft phases of the multi-phase steels. As a result, as far as the specimen steels of the present study were concerned, the estimated average hardness was close to that of ferrite. The data of part (a) of Fig. 6 were rearranged according to the estimated hardness of the soft phase into the graph in part (b); this graph shows close correlation between the strain rate sensitivity of flow stress and the hardness of the soft phase plotted along the abscissa. This result indicates that, even with steels consisting of two or more phases, the parent phase, ferrite, primarily governs deformation characteristics in a range of high strain rate. The graph also shows that multi-phase steels exhibit better strain rate sensitivity than single-phase steels of the same quasi-static strength. This indicates that strengthening using soft and hard phases such as those of dual-phase and transformation-induced plasticity steels is suitable for steels for applications to the structural members of crumple zones.

3.2 Evaluation of work hardening characteristics in a high-strain range

3.2.1 Evaluation by the simple shear test

Next, material properties in a large-strain range were examined.

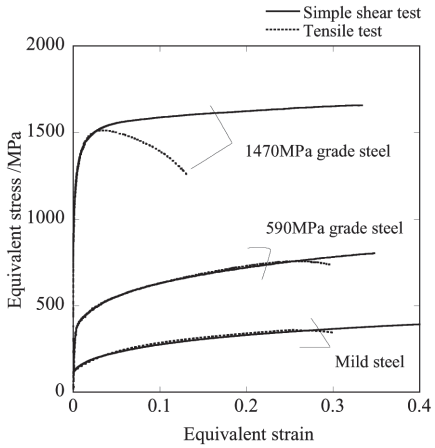

Fig. 7 Equivalent stress-strain curves

Test pieces of three steel grades (a mild steel and 590- and 1,470-MPa steels) were subjected to a uniaxial tensile test and simple shear test,[21] and the results of the simple shear test were converted into an equivalent stress-strain curve under the isotropic hardening hypothesis (the von Mises rule). **Fig. 7** shows the results of the simple shear test after the conversion together with those of the tensile test. Compared with the tensile test results, stress did not fall drastically but mostly increased monotonously in the simple shear test; this was true even with the 1,470-MPa grade steel, which exhibits low uniform elongation. This indicates that, since the material properties as evaluated through tensile test include apparent fall of stress due to necking and other factors, use of tensile test results without modification for collision analysis may lead to results that do not correctly reflect the real material properties and spoil the analysis accuracy.

3.2.2 Evaluation by the correction of uniaxial tensile test results by applying FEM analysis

Necking is likely to occur at an early stage of the high-speed tensile test because heat is generated by plastic deformation,[22] and as a consequence, strength becomes uneven within a test piece. **Fig. 8** (a) shows the results of quasi-static and high-speed tensile tests of mild steel. The graph includes the results of the cases where 8% and 16% prestrains were applied quasi-statically to the test pieces for the high-speed tensile test (curves 2 and 3, respectively). When test pieces deformed at a strain rate of 1,000 s^{-1} from the beginning, stress decreased immediately after reaching an initial peak. In contrast, with prestrain, the curves were generally on the high-stress side of that without prestrain. Most likely, this is merely an apparent phenomenon resulting from necking at an early stage under a high strain rate.[27]

In view of the above, applying coupled analysis of heat generation and structural change, the authors calculated the apparent stress decrease due to necking from the stress-strain curve.[22] As a result, the curves of the test pieces with prestrain became closer to those without prestrain, and the curves tended to converge on a single curve regardless of the application or otherwise of prestrain (see Fig. 8 (b)). This indicates that even in high-speed deformation, when the effects of necking are adequately removed, it is possible to correctly measure the increase in stress as deformation advances.

From these results, the following can be said about the forming characteristics of steel sheets. (1) The strain rate sensitivity of flow stress changes depending on the strengthening mechanism applied

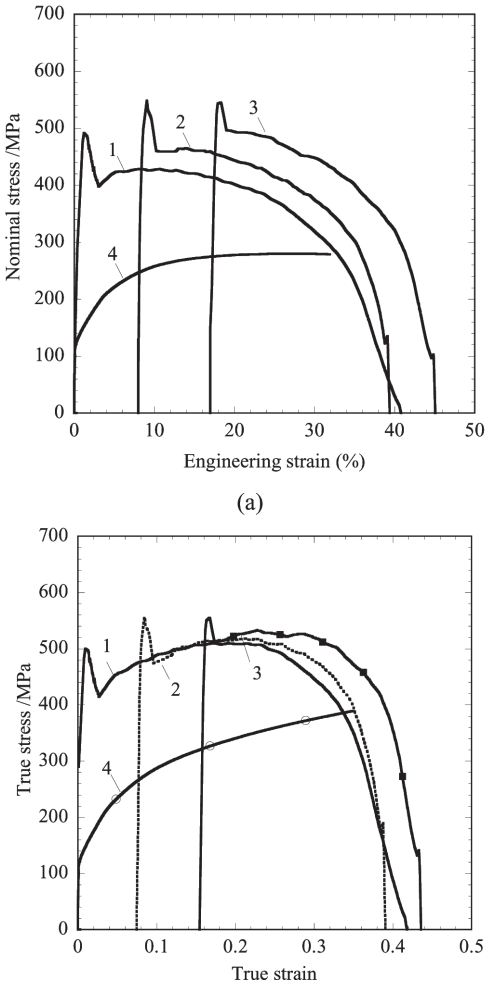

Fig. 8 Stress-strain curves

to the steel in question. (2) In a strain rate from 0.001 to 1,000 s^{-1}, flow stress increases with strain. While various material models have been proposed for application to collision analysis and in consideration of the current limitations of analysis codes and practicality of test methods, approximating the stress-strain curve of uniaxial tensile test using Equation (1), which applies the Swift rule to work hardenability and the Cowper-Symonds rule to the strain rate sensitivity, is considered appropriate as a material model for collision analysis.

4. Change of Material Properties at Paint Baking during Manufacture of Car Bodies

It has been well known that work hardening and thickness change during press forming of steel sheets have effects on collision performance of the formed parts, and many studies have reported on coupled analysis of forming and collision aiming at reflecting them in collision analysis to improve accuracy.[28] In addition, when steel sheets that are expected to harden at paint baking (bake hardening) are used, it is necessary to employ a method that takes bake hardening into consideration in collision analysis. Bake hardening is considered to result from the following points. Carbon in steel diffuses at paint baking temperatures to immobilize mobile dislocations that

were formed during press forming, and the stress required to cause reyielding increases. Bake-hardening sheets have been used for outer body panels to improve dent resistance, but sometimes high bake hardening effects are also obtained with high-strength sheets for body structural use depending on steel grade and manufacturing method. For efficient design work of car bodies to increase strength and reduce weight, it is necessary to accurately predict the hardening behavior of steel sheets during press forming and paint baking.

It is widely known that, while the initial plastic anisotropy of annealed single-phase, polycrystalline metal material depends mainly on crystal orientation distribution, that of a material having undergone a significant prestrain is affected more by the dislocation structures within crystal grains resulting from deformation than by the change in crystal orientation.[29] In view of this, on the basis of the observation of intra-grain cell structures under strain path change, Teodosiu et al.,[30] though in a semi-phenomenological manner, worked out an anisotropic hardening model based on dislocation structure, making it possible to precisely predict cross hardening and the Bauschinger effect under the condition of orthogonal strain paths. In addition, Suzuki et al.[31] applied the Teodosiu model to a widely used general-purpose finite element code; therefore, successfully enhanced the accuracy of sheet forming simulation.Meanwhile, the past knowledge of the strain path dependency of bake hardening has not gone beyond being phenomenological but dwelt mainly on the change of formability due to aging,[32] and there have been no studies associating the characteristics of work-induced anisotropy due to strain path change with the anisotropy of bake hardening. In consideration of this, the authors applied uniaxial tensile prestrain to bake-hardening sheets, investigated how in-plane anisotropy of the uniaxial tensile yield stress would change before and after heat treatment; therefore, studied a collision analysis method taking into consideration work history during press forming and bake hardening during painting.[33]

Test pieces were cut out from sheets of bake-hardening steel with a thickness of 0.7 mm and of a 340-MPa class, a primary tensile deformation of 2 or 6% was applied to them in the rolling direction as shown in **Fig. 9**; then, as a secondary deformation, tensile test was conducted at 0 to 90° to the rolling direction at intervals of 15° (angle α in Fig. 9). To investigate bake-hardening properties under strain path change, some of the test pieces underwent an additional heat treatment at 170°C for 20 min (aging) between the primary and secondary deformations.

Fig. 10 shows in-plane anisotropy of yield stress after prestrain by uniaxial tension.[34] It is clear from the graph that, while the yield stress of steel sheets generally increases through working, the increase being strongly anisotropic, the hardening through paint baking (aging) mitigates the anisotropy of the yield stress of prestrained specimens or homogenizes the yield stress. Therefore, in the collision analysis of painted and baked car bodies, it is not necessary to introduce a new constitutive model of materials, but rather, it is sufficient for better approximation of stress-strain relations to simply

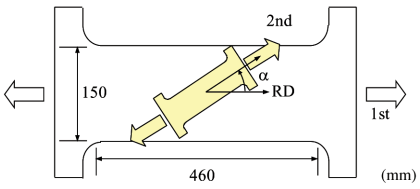

Fig. 9 Experimental procedure

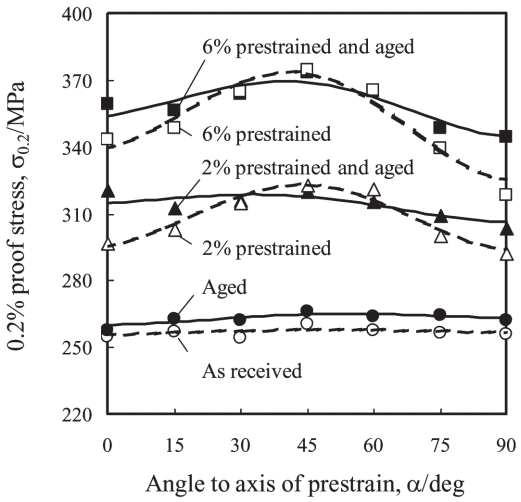

Fig. 10 Anisotropy of work hardening after strains in different directions and effects of bake hardening (aging)[34]

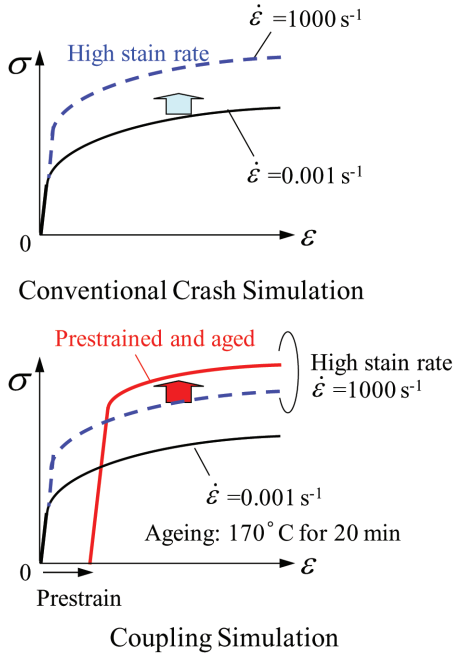

Fig. 11 Crash analysis method for prestrained and aged steel structure

add bake hardening amount determined by a common method uniformly onto the work hardening curve of the material in question, according to the conventional isotropic hardening model widely used in industrial practice (see **Fig. 11**). However, it should to be noted that with mild steel, which has low bake hardenability, strain path change causes notable plastic anisotropy; for this reason, a constitutive model of materials capable of accounting for anisotropic hardening behavior such as the Teodosiu model[30] is more desirable.

5. Conclusions

Collision analysis is indispensable for the collision safety design of car bodies. This report has presented the following as the approaches from the material side to enhance the prediction accuracy of collision analysis: optimum test piece geometry for accurate

evaluation of the strain rate sensitivity of flow stress of ultra-high-strength steel sheets of tensile strength exceeding 1,500 MPa; the mechanism through which the strain rate sensitivity becomes manifest; a material model for collision analysis that enables accurate approximation of stress-strain curve; and the anisotropy of bake hardening properties in paint baking.

The Nippon Steel Corporation will continue developing new solutions from the material side, such as fracture prediction, in response to the ever increasing need for further enhancement of collision safety design of car bodies.

References

1) Yokoyama, A. et al.: J. of JSAE. 65 (1), 59 (2011)
2) Yonemura, S. et al.: Proc. of JSAE Meeting. 21 (07), 1 (2007)
3) Yoshida, H. et al.: Zairyou no Shougeki Mondai Symposium Kouen Ronbunshu (Proc. Symposium on Impact Problems of Material). 8, 65 (2005)
4) Marciniak, Z. et al.: Mechanics of Sheet Metal Forming. Edward Arnold, 1992, p. 62
5) Lemaitre, J.: A Course on Damage Mechanics. Berlin, Springer-Verlag, 1992
6) Uenishi, A. et al.: IBEC'96 Interior & Safety Systems. 1996, p. 89
7) Uenishi, A. et al.: Sosei Kako Symposium (Plastic Working Symposium). 258, 31 (2007)
8) Kolsky, H.: Proc. Phys. Soc. B62, 676 (1949)
9) Hopkinson, B.: Phil. Trans. A. 213, 437-452 (1914)
10) Hayashi, T. et al.: Shougeki Kougaku (Impact Engineering). Nikkan Kogyo Shimbun, Ltd., Tokyo, 1988
11) Rodriguez, J. et al.: J. De Physique IV, 4 (8), C8-83 - C8-88 (1994)
12) Sakui, S. et al.: J. of Japan Institute of Metals. 28 (9), 537 (1964)
13) Hirose, S. et al.: Proc. Japanese Spring Conf. for Technology of Plasticity. 141 (2008)
14) Hirose, S. et al.: Proc. Japanese Joint Conf. for Technology of Plasticity. 59, 413 (2008)
15) JRI Solutions Ltd: LS-Dyna ver.971 User's Manual. Volume I. 2007
16) Fukui, S. et al.: RIKEN Hokoku (Tech. Report of RIKEN). 41 (1), 5 (1965)
17) Yoshida, S. et al.: RIKEN Hokoku. 39 (3), 137 (1963)
18) von Karman, T., Duwez, P.: J. Appl. Phys. 21 (8), 987 (1950)
19) Fukui, S. et al.: Report of Aeronautical Research Institute, Univ. of Tokyo. 3 (6), 361 (1963)
20) ISO 26203-1:2010, Tensile Testing at High Strain Rates —Part 1: Elastic-bar-type systems
21) Suzuki, N. et al.: J. Japan Society for Technology of Plasticity. 46 (534), 636 (2005)
22) Uenishi, A. et al.: Int. J. Plasticity. 20, 915 (2004)
23) Uenishi, A. et al.: Proc. of JSAE Meeting. 15 (9), 17 (2009)
24) Uenishi, A. et al.: Acta Materialia. 51, 4437 (2003)
25) Kawata, K. et al.: Institute of Physics, Conference Series. 1979
26) Uenishi, A. et al.: J. Japan Society for Technology of Plasticity. 46 (534), 646 (2005)
27) Kuroda, M. et al.: Int. J. Solids and Structures. 43, 4465 (2006)
28) Hiwatashi, S. et al. Proc. of JSAE Meeting. 21 (7), 13 (2002)
29) Rauch, E.F. et al.: Mater. Sci. Eng. 113, 441 (1989)
30) Teodosiu, C. et al.: Proc. Numiform'95. 1995, p. 173
31) Suzuki, N. et al.: J. Japan Society for Technology of Plasticity. 46 (534), 636 (2005)
32) Jun, G., Hosford, W.F.: Metall. Trans. A. 17A, 371 (1986)
33) Yonemura, S. et al.: Proc. of JSAE Meeting. 15 (9), 17 (2009)
34) Yonemura, S. et al.: Tetsu-to-Hagané. 92 (9), 516 (2006)

Satoshi HIROSE
Senior Researcher, Ph.D.
Forming Technologies R&D Center
Steel Research Laboratories
20-1 Shintomi, Futtsu, Chiba 293-8511

Shigeru YONEMURA
Senior Researcher, Dr.Eng.
Kimitsu R&D Lab.

Akihiro UENISHI
Chief Researcher, Dr.
Sheet Products Lab.
Steel Research Laboratories

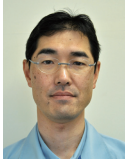

Shunji HIWATASHI
Chief Researcher, Ph.D.
General Manager
Nagoya R&D Lab.